32nd Annual International Conference of the IEEE EMBS
Buenos Aires, Argentina, August 31 - September 4, 2010

# Local Image Enhancement for Fiducial Marker Detection in Electronic Portal Images of Prostate Radiotherapy

Patrick Bonneau[1], Alexandra Branzan Albu[1], and Michelle Hilts[2]

[1] Dept. of ECE, University of Victoria, Canada, [2]BC Cancer Agency, Victoria, Canada
pbonneau@ece.uvic.ca, aalbu@uvic.ca, mhilts@bccancer.bc.ca

## Abstract

**This paper proposes a new method for the automatic contrast enhancement of fiducial markers in low-radiation Electronic Portal Images. It is shown that the proposed approach significantly enhances the contrast of the fiducial markers and produces results where these markers are clearly visible. The main theoretical contribution consists in designing an algorithm that enhances the contrast of small structures in noisy images; the parameters of this algorithm are not empirically selected, but determined via a maximum search over a contrast metric. From a practical standpoint, the proposed method has direct applications in the current clinical workflow involving manual marker detection. It is also able to significantly improve the performances of automatic marker detection reported in literature.**

## 1. Introduction

Image guided radiation therapy (IGRT) is a new type of external therapy relying on image guidance for delivering lethal doses of radiation to cancerous tissue, while ensuring that the surrounding healthy structures are sheltered from radiation. IGRT is particularly well suited for the treatment of prostate cancer.

In the external radiation of prostate cancer, the most significant error occurs in the spatial delivery of the radiation dose due to the variability of the patient position. IGRT aims at minimizing this source of error by verifying the prostate location using electronic portal images acquired with low radiation prior to each treatment session. Position set-up errors are determined by matching the prostate location in the portal image to that in digitally reconstructed radiographs.

Since the prostate is not visible in portal images, its position is computed using fiducial markers implanted into the prostate. These markers are more radio-opaque than soft tissue and therefore they are more visible in portal images. The 3D coordinates of each marker are computed from 2 portal images acquired at anterior and lateral views respectively. The visual identification of markers on portal images is not trivial, mainly due to the low contrast and signal to noise ratio of the EPI images.

The manual detection of fiducial markers is tedious and time consuming. This motivates the development of image processing techniques for automated detection. Most proposed techniques rely on template matching with kernels that are constructed using a priori knowledge about the marker geometry and size. Nederveen et al [1] used a rectangular marker extraction kernel (MEK) for modeling the appearance of cylindrical fiducial markers. Buck et al [2] used a Mexican hat filter (MHF) to identify spherical markers. Aubin et al [3] convolve unit ring and unit cercle templates with a predefined search region in order to create a "contrast" image; large values in the "contrast" image signal locations where marker shapes are found.

Other techniques rely upon a manual initialization of the automatic detection process. For instance, Balter et al [4] created marker reference images from the manually segmented portal images corresponding to the first day of treatment. These reference images are cross-correlated with images from subsequent days, in order to detect the pixels with the highest correlation.

In an interesting comparative study, Harris et al [5] implemented the automatic detection methods in [1-4] and compared them on the same image database. They concluded that none of these methods meets clinical performance criteria for fully automated marker detection. The cross-correlation technique using manual initialization gave best results.

Reasons for the limited performance of the fully automatic detection methods of marker detection are similar to the challenges encountered in the manual identification process (poor contrast, poor signal to noise ratio, presence of bony structures). As shown in [5], current clinical practice involves team-based

evaluations of difficult images, as well as image filtering with empirical, user-defined parameters.

To improve the performance of automatic marker detection, as well as the clinical workflow of manual detections, we propose a systematic approach for image enhancement applied to portal images of prostate radiotherapy. Our main contribution lies in the automatic computation of all parameters of the approach via optimization; there are no arbitrary or empirical set-ups of parameters in our approach. The reminder of this paper is structured as follows. Section 2 provides a description of the approach. Section 3 discusses experimental results, while section 4 draws conclusions and outlines future work.

## 2. Proposed approach

Fig. 1 presents a modular diagram of the proposed approach, where the results of each processing step are visualized on a typical sample image from the experimental database. *One may note that the original contribution does not lie in the proposal of new algorithms for contrast enhancement and/or noise removal, but on the optimization of the parameter selection process for these two blocks.* The parametric optimization approach is described after a brief description of all processing blocks.

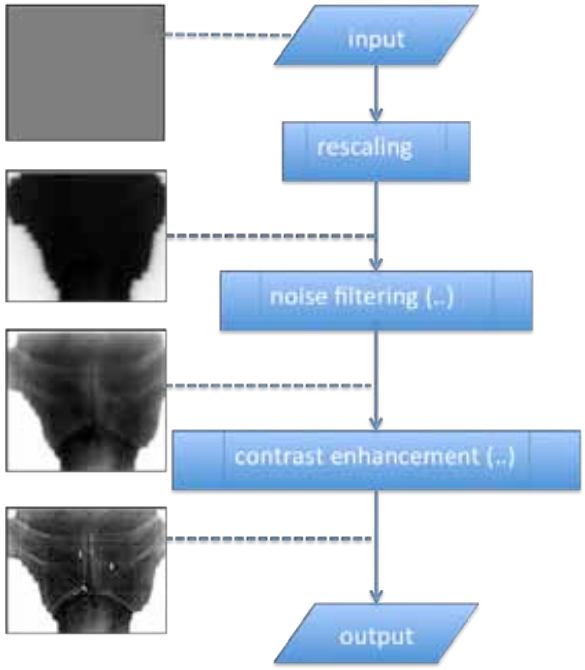


**Fig. 1. Diagram of the proposed approach. Parametric processing blocks are shown as *process_name (..)***

### 2.1. Rescaling

As shown in Fig. 1, the input image shows no structural/marker information. This is because the brightness levels in the original image are concentrated in less than 3% of the gray level range. Out of 65536 available gray levels for 16 bit input images, the information is encoded only on gray levels located inside the [32000-34000] range. Histogram equalization induces distortions on the edges of the field of treatment. In order to preserve these edges, we have adopted a linear rescaling solution.

### 2.2. Noise filtering

Noise amplification is a typical side-effect of contrast enhancement. Thus, noise removal is usually implemented as a low-pass filter (LPF) prior to contrast enhancement. However, this standard approach does not work well for the task at hand. The small size of markers is very close to the size of noise-induced artifacts and thus it is possible to 'erase' an marker by applying low-pass filtering. We use therefore a homomorphic filter, which affects the low and high frequency components in different, controllable ways. A homomorphic filter can be described as the weighted sum of a low-pass filter and a high-pass filter. Therefore, the parameters of this filter are the weights $\gamma_{HP}$ and $\gamma_{LP}$ of the two filters; these parameters are set to optimal values, as described later in this section. The high-pass filter and the low-pass filter are implemented as unit-gain Butterworth filters with ($\omega_c$=0.0039, n=52) and ($\omega_c$=0.11, n=33) respectively.

Fig. 1 shows that the output of the noise filtering module starts revealing the bony anatomy and the fiducial markers. However, the image is blurred, which is why contrast enhancement is further needed.

### 2.3. Contrast enhancement.

This processing block is based on the Deng et al [6] technique for log-ratio enhancement. The choice of this technique is based on its ability to enhance simultaneously the overall image contrast and the sharpness of the edges. Therefore, it is suitable for revealing both fiducial markers and the bony anatomy in portal images. The adopted technique is described by equation (1).

$$F'(x,y) = (A(x,y) \oplus \beta) \oplus (\alpha \otimes (F(x,y) \Theta A(x,y))) \quad (1)$$

where $F(x,y)$ and $F'(x,y)$ represent the logarithms of the input and output images respectively, and $A(x,y)$ is the blurred version of $F(x,y)$. The symbols $\oplus$, $\Theta$ and $\otimes$ denote operators for logarithmic addition, subtraction and multiplication.
Parameters $\beta$ and $\alpha$ control the weight of the low-frequency component $A(x,y)$ and the high-frequency component $F(x,y)\,\Theta\,A(x,y)$ of the enhanced image respectively.

### 2.4. Parameter optimization

The proposed algorithm for automatic contrast enhancement has four parameters, namely $\gamma_{LP}$ and $\gamma_{HP}$ for noise removal, and $\beta$ and $\alpha$ for the log-ratio enhancement. Due to the large variability in image properties, it is impossible to find empirically a unique set of parameters to work for the entire database. It is desirable to achieve an automatic selection of the values of the parameters. Therefore, we adopt the *LogAMEE* metric for contrast proposed by Panetta et al [7]. This metric was selected after careful consideration of several other contrast metrics due to the fact that it returned maxima that were consistent with human evaluations of good contrast.
The LogAMEE metric represents the average contrast entropy for the $k_1$x$k_2$ image block, where the contrast is defined by the Michelson law.

$$LogAMEE = \frac{1}{k_1 k_2} \otimes \sum_{i=1}^{k_1} \sum_{j=1}^{k_2} \frac{I^w_{\max:k,l} \Theta I^w_{\min:k,l}}{I^w_{\max:k,l} \oplus I^w_{\min:k,l}} \otimes \ln \frac{I^w_{\max:k,l} \Theta I^w_{\min:k,l}}{I^w_{\max:k,l} \oplus I^w_{\min:k,l}} \qquad (2)$$

The symbols $\oplus$, $\Theta$ and $\otimes$ denote operators for logarithmic addition, subtraction and multiplication.
To find optimal parametric values, we consider the contrast metric first as a function of $\gamma_{LP}$, $\gamma_{HP}$, and next as a function of $\beta$, $\alpha$, as follows:

$$(\gamma_{HP},\gamma_{LP}) = \underset{\substack{1<\gamma_{HP}<1.5 \\ 0<\gamma_{LP}<1}}{\arg\max}\, LogAMEE(\gamma_{HP},\gamma_{LP})$$
$$(\alpha,\beta) = \underset{\substack{1<\alpha<20 \\ 0.35<\beta<0.5}}{\arg\max}\, LogAMEE(\alpha,\beta) \qquad (3)$$

The range of values considered for ($\gamma_{HP}$, $\gamma_{LP}$) and ($\alpha$ , $\beta$) is consistent with recommendations in [7]. Fig. 2 shows examples of computations of optimal values for ($\gamma_{HP}$, $\gamma_{LP}$) , and for ($\alpha$ , $\beta$).

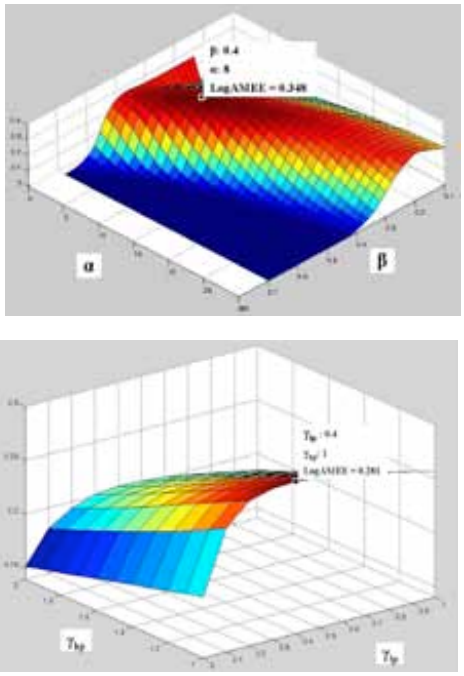


**Fig. 2. Example of determination of ($\alpha$ , $\beta$) and ($\gamma_{HP}$, $\gamma_{LP}$) optimal values through maxima search**

## 3. Experimental results

The proposed approach has been tested on a database consisting of electronic portal images acquired from 9 patients (37 images per patient) prior to radiation therapy sessions. The portal images were acquired at a low radiation level of 6 MV. The fiducial markers (Best Medical International Inc., Springfield, VA) used in this study were cylindrical gold seeds, 2 mm in diameter and 5 mm in length. In portal images, these markers are shown as linear structures of various orientations and a maximum length of 9 pixels.
The degree of contrast enhancement achieved by the proposed approach was measured using the Weber ratio, $c = I_{\max} - I_{\min} \big/ I_{average}$ .
This measure is different from the one used in the parametric selection process because the contrast enhancement is to be measured locally, in the vicinity of each fiducial marker. The Weber ratio was chosen for its simplicity and its compatibility to local measurements within regions comparable in size with the markers. The local measurement of contrast was restricted to square regions of 9x9 pixels centered on each fiducial marker.
Fig. 3 provides examples of results of contrast enhancement, presented in a before-after manner.

Table 1 summarizes the statistics (average and standard deviation) that were computed over the entire database. These statistics are reported on a per patient basis, since image characteristics vary significantly among patients. The input image is homogeneous, thus has is no contrast measure associated to it. The contrast is measured after linear rescaling, noise removal, and log-ratio enhancement. Intermediate results are shown in order to quantify the contribution of each processing module to the final result. One may note that significant improvements in contrast have been obtained for all patients and for both views.

## 4. Conclusions

This paper proposes a new method for the automatic contrast enhancement of fiducial markers in low-radiation EPI images. The proposed approach significantly enhances the contrast of the fiducial markers and produces results where these markers are clearly visible. The main contribution consists in designing an algorithm that enhances the contrast of small objects with parameters optimized via a maximum search over a contrast metric. Ongoing work concentrates upon the automatic segmentation of the FM seeds from the enhanced images.

**Table 1. Statistics for contrast enhancement results (left lateral view and anterior view)**

| Patient | Left lateral view | | | | | | Anterior view | | | | | |
|---|---|---|---|---|---|---|---|---|---|---|---|---|
| | Rescaling | | Noise filtering | | Final | | Rescaling | | Noise filtering | | Final | |
| | Average | STD | Average | STD | Average | STD | Average | STD | Average | STD | Average | STD |
| 1 | 0,346 | 0,176 | 0,884 | 0,336 | 1,007 | 0,326 | 0,723 | 0,300 | 1,755 | 0,694 | 1,960 | 0,770 |
| 2 | 0,563 | 0,150 | 1,122 | 0,300 | 1,295 | 0,324 | 1,218 | 0,358 | 1,844 | 0,454 | 1,902 | 0,358 |
| 3 | 0,631 | 0,160 | 1,13 | 0,257 | 1,143 | 0,199 | 1,157 | 0,362 | 2,482 | 0,900 | 2,498 | 0,940 |
| 4 | 0,49 | 0,130 | 1,202 | 0,290 | 1,239 | 0,243 | 0,907 | 0,199 | 2,255 | 0,562 | 2,443 | 0,355 |
| 5 | 0,092 | 0,019 | 0,229 | 0,071 | 0,412 | 0,131 | 0,228 | 0,054 | 0,699 | 0,175 | 0,977 | 0,228 |
| 6 | 0,323 | 0,036 | 0,836 | 0,126 | 0,998 | 0,163 | 0,904 | 0,390 | 2,029 | 0,774 | 1,935 | 0,561 |
| 7 | 0,348 | 0,129 | 0,9 | 0,297 | 1,0696 | 0,346 | 0,678 | 0,300 | 2,060 | 1,184 | 2,215 | 1,236 |
| 8 | 0,533 | 0,156 | 1,33 | 0,426 | 1,345 | 0,357 | 1,350 | 0,358 | 2,557 | 0,546 | 2,565 | 0,441 |
| 9 | 0,407 | 0,305 | 1,001 | 0,441 | 1,08 | 0,489 | 1,0811 | 0,535 | 2,0984 | 0,849 | 2,1380 | 0,665 |

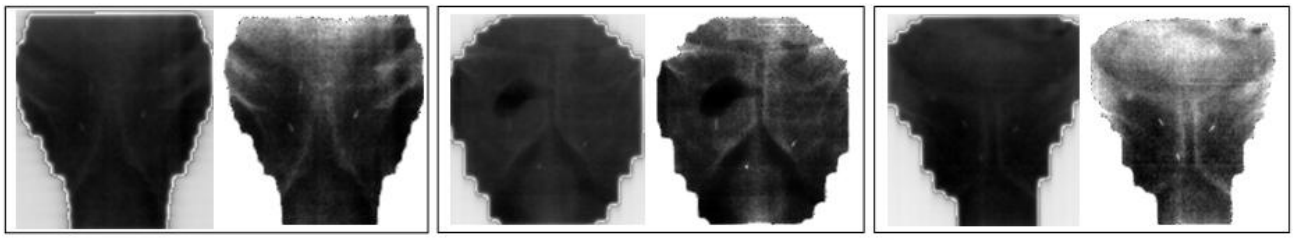

**Fig. 3. Examples of results obtained with the proposed contrast enhancement approach**

## 5. References


[1] A. J. Nederveen, J.J.W. Lagendjik, and P. Hofman, "Feasibility of automatic marker detection with an a-Si flat panel integer," *Physics in Medicine and Biology*, 46, pp. 1219-1230, 2001.

[2] D. Buck, M. Alber, F. Nusslin, "Potential and limitations of the automatic detection of fiducial markers using an amorphous silicon flat-panel imager," *Phys. in Med. and Biol.*, 48, pp. 763-764, 2003.

[3] S. Aubin, L. Beaulieu, S. Pouliot, et al, "Robustness and precision of an automatic marker detection algorithm for online prostate daily targeting using a standard V-EPID," Medical Physics, 30(7), pp. 1825-1833, 2003.

[4] J. Balter, K.L. Lam, H.M. Sandler, et al, "Automated localization of the prostate at the time of treatment using implanted radiopaque markers," *Int. J. of Radiation Oncology, Biology, Physics,* 33, pp. 1281-1286, 1995.

[5] E.J. Harris, H.A. McNair, and P.M.Evans, "Feasibility of fully automated detection of fiducial markers implanted into the prostate using electronic portal imaging: a comparison of methods," *Int. J. of Radiation Oncology, Biol., Phys.,* 66(4), pp. 1263-1270, 2006.

[6] G. Deng, L. Cahill, and G.R. Tobin, "The study of logarithmic image processing model and its application to image enhancement," *IEEE Trans. on Image Proc*., 4, pp. 506-512, 1995.

[7] K.A. Panetta, E.J. Wharton, and S.S. Agaian. "Human visual system-based image enhancement and logarithmic contrast measure," *IEEE Trans. on Systems, Man, and Cybernetics*, 38(1), pp. 174-188, 2008.